[15] R. H. Schuler, P. Neta, H. Zemel, R. W. Fessenden, *J. Am. Chem. Soc.* **1976**, *98*, 3825 – 3831.
[16] D. J. Deeble, S. Das, C. von Sonntag, *J. Phys. Chem.* **1985**, *89*, 5784 – 5788.
[17] H. M. Novais, S. Steenken, *J. Am. Chem. Soc.* **1986**, *108*, 1 – 6.
[18] S. Steenken, J. P. Telo, H. M. Novais, L. P. Candeias, *J. Am. Chem. Soc.* **1992**, *114*, 4701 – 4709.
[19] L. P. Candeias, P. Wolf, P. O'Neill, S. Steenken, *J. Phys. Chem.* **1992**, *96*, 10302 – 10307.
[20] L. P. Candeias, S. Steenken, *J. Phys. Chem.* **1992**, *96*, 937 – 944.
[21] S. Fujita, S. Steenken, *J. Am. Chem. Soc.* **1981**, *103*, 2540 – 2045.
[22] The total yield of $TMPD^{\bullet+}$ was 100% as calibrated by the reaction of TMPD with $(SCN)_2^{\bullet-}$, whose yield (in 10 mM KSCN) is equal to that of $^{\bullet}OH$, see: R. H. Schuler, L. K. Patterson, E. Janata, *J. Phys. Chem.* **1980**, *84*, 2088.
[23] From the dependence on [TMPD] of the rate of formation of $TMPD^{\bullet+}$ in the initial direct, "fast" reaction the rate constant for its formation by $^{\bullet}OH$ is $1.0 \times 10^{10}\,M^{-1}s^{-1}$. The same value was obtained from an experiment where 2-propanol competed with TMPD for $^{\bullet}OH$ (with $k(^{\bullet}OH + i\text{PrOH}) = 2.2 \times 10^{9}\,M^{-1}s^{-1}$).
[24] All rate constants given in the paper refer to $(20 \pm 0.2)^{\circ}C$.
[25] The time-resolved AC method was used. Dosimetry was performed with the reaction $^{\bullet}OH$ and *N,N*-dimethylaniline which yielded *N,N*-dimethylaniline$^{\bullet+}$ and OH^-: J. Holcman, K. Sehested, *J. Phys. Chem.* **1977**, *81*, 1963.
[26] This also shows that $TMPD^{\bullet+}$ does not react with OH^-, as also concluded from the independence of the lifetime of $TMPD^{\bullet+}$ on $[OH^-]$.
[27] In contrast, the absorption at 350 nm was much higher than that at pH 7 – 8 (cf. insets a, b in Figure 1).
[28] Using 0.2 – 0.5 mM TMPD and 0.4 – 0.5 M KOH.
[29] P. Neta, R. H. Schuler, *Radiat. Res.* **1975**, *64*, 233.
[30] See, for example: S. Steenken and V. Jagannadham, *J. Am. Chem. Soc.* **1985**, *107*, 6818, and references therein.
[31] For calibration an N_2O-saturated solution of 10 mM sodium formate and 0.5 mM MV^{2+} was used (yield of $MV^{\bullet+} \equiv 100\%$).
[32] As calibrated by reaction with $(SCN)_2^{\bullet-}$. However, the total yield of radical cation was less than 100%, indicating H-abstraction from terminal carbon atoms in the alkyl groups.
[33] In the case of tetra*ethyl*-*p*-phenylenediamine, the activation parameters were measured for the intramolecular formation of radical cation: $\Delta H^{\neq} = 6.2\ \text{kcal mol}^{-1}$, $\Delta S^{\neq} = -19\ \text{cal mol}^{-1}\,K^{-1}$.
[34] Alkyl substitution at C_α leads to stabilization of the radical and thus disfavors the transformation to the aromatic radical cation.
[35] With $k_{\text{elimination}} \geq 3 \times 10^6\ s^{-1}$.
[36] S. Steenken, *J. Chem. Soc. Faraday Trans. 1* **1987**, *83*, 113 – 124.
[37] The conceivable alternative that the radical which undergoes the transformation reaction to $TMPD^{\bullet+}$ is the *ipso*-OH adduct, is thereby excluded, since the yield of the *ipso*-OH adduct would *de*crease on going from $^{\bullet}OH$ to $O^{\bullet-}$.
[38] The thermodynamic acidity of $TMPD^{\bullet+}$ is not known. However, on the basis of the observation that even in 1M KOH, $TMPD^{\bullet+}$ persists, its pK_a value is estimated to be $\gg 14$ which is in line with the conjugate base, $>NCH_2^{\bullet}$, being protonatable by H_2O.
[39] The conversion of $>NCH_2^{\bullet}$ into $TMPD^{\bullet+}$ can be accelerated by phosphate: For this reaction at pH 8, $k = 2 \times 10^6\,M^{-1}s^{-1}$ (determined from the linear dependence of k_{obs} on [phosphate]).
[40] E. Baciocchi, M. Bietti, O. Lanzalunga, *Acc. Chem. Res.* **2000**, *33*, 243 – 251.
[41] The basis for the electron transfer from the ring to the side chain lies in the very high electron density at the ring which is enhanced through the second dialkylamine function. In line with this, the reaction corresponding to that in Scheme 2 does not take place for the analogous α-aminoalkyl radical of *N,N*-dimethylaniline.
[42] R. H. Schuler, A. L. Hartzell, B. Behar, *J. Phys. Chem.* **1981**, *85*, 192 – 199.

Liquid-Phase Synthesis of Colloids and Redispersible Powders of Strongly Luminescing $LaPO_4$:Ce,Tb Nanocrystals**

Karsten Riwotzki, Heike Meyssamy, Heimo Schnablegger, Andreas Kornowski, and Markus Haase*

An increasing number of nanocrystalline materials have been synthesized in high-boiling coordinating solvents, since binding of the solvent molecules to the particle surface leads to colloidal solutions of well-separated particles.[1] If process parameters such as concentration and temperature are properly adjusted[2] and, most importantly, a suitable solvent for the reaction is found, colloidal solutions of highly crystalline nanoparticles with very narrow particle size distributions are the result. Examples for this method are the synthesis of high-quality cadmium chalcogenide nanoclusters[1a] and TiO_2 nanoclusters[1b] in trioctylphosphine oxide (TOPO) and the preparation of InP[1c,d] and InAs nanoclusters[1e] in trioctylphosphane (TOP). Similarly, ZnSe,[1f] Fe_2O_3, Mn_3O_4, and Cu_2O nanoclusters[1g] have been prepared in long-chain alkylamines. Our synthesis of $LaPO_4$:Eu and $CePO_4$:Tb in tris-ethylhexylphosphate[1h] shows that the method is also applicable to *doped* nanoparticles.

Oxide materials form the active material of most solid-state lasers and are technologically important as phosphors in cathode ray tubes, X-ray detectors, and in lighting applications.[3] The latter group includes the mixed phosphate $La_{0.40}Ce_{0.45}Tb_{0.15}PO_4$, which is used in luminescent lamps as highly efficient emitter of green light.[4] The material is chemically very stable, even in the presence of the mercury plasma discharge inside the lamp, and has an overall luminescence quantum yield of 93%.[5] Redispersible nanoparticles of $La_{0.40}Ce_{0.45}Tb_{0.15}PO_4$ may therefore form a stable and efficient substitute for organic laser dyes in various applications. In fact, semiconductor nanoparticles such as CdSe have successfully been applied, for instance, as luminescing labels for biomolecules[6] and as light-emitting molecular substances in electroluminescent devices.[7]

Herein we present an improved synthesis that yields more than 10 grams of the ternary system $La_{0.40}Ce_{0.45}Tb_{0.15}PO_4$ in a simple one-pot reaction which does not involve rapid mixing of dissolved compounds. Rapid mixing at elevated temperatures is often applied to separate nucleation and growth of the nanoparticles,[8] but becomes increasingly difficult with larger amounts of reactants. Nevertheless, our procedure yields a remarkably narrow particle size distribution even on this preparative scale. This is shown by transmission electron

[*] Dr. M. Haase, K. Riwotzki, H. Meyssamy, Dr. H. Schnablegger, A. Kornowski
Institut für Physikalische Chemie
Universität Hamburg
Bundesstrasse 45, 20146 Hamburg (Germany)
Fax: (+49) 40-42838-3452
E-mail: haase@chemie.uni-hamburg.de.

[**] This work was supported by the Deutsche Forschungsgemeinschaft (DFG). We thank S. Bartholdi-Nawrath for help with the electron micrographs and J. Kolny for measuring the powder X-ray diffraction data.

  1433-7851/01/4003-0573 $ 17.50+.50/0

micrographs (TEMs, Philips CM 300 UT electron microscope) given in Figure 1. The TEM images further show that the nanoparticles have a mean diameter of 5 to 6 nm and that their shape varies from almost spherical to ellipsoidal with

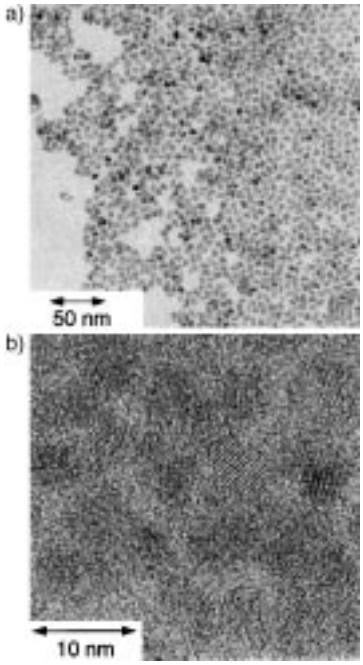

Figure 1. a) TEM image of $LaPO_4$:Ce,Tb nanoparticles. b) High-resolution TEM image of the particles.

aspect ratios of up to two. Many particles display well-defined edges, indicating faceting of these crystallites. High crystallinity is also inferred from the high-resolution TEM images of the material (Figure 1b) showing lattice fringes for most particles and from the powder X-ray diffraction (XRD) data given in Figure 2. Figure 2 displays not only the measured

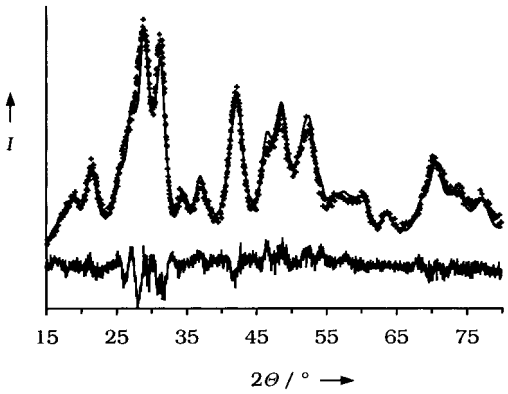

Figure 2. X-ray powder diffraction data (+), Rietveld fit (solid line through data points), and difference curve (solid line below data points) of $LaPO_4$:Ce,Tb nanoparticles.

XRD pattern (for clarity, only every second data point (+) is given), but also a simulation of the XRD pattern based on the Rietveld method[9] (line through data points) and the difference curve between the XRD data and the Rietveld fit. The numerical values used in the Rietveld simulation (Table 1)

Table 1. Results of the Rietveld fit given in Figure 2 and unit cell parameters of the $LaPO_4$:Ce,Tb nanoparticles as well as of bulk $CePO_4$ and $LaPO_4$.

	Nanoparticles	Bulk $LaPO_4$	Bulk $CePO_4$
space group (no.)	$P12_1/n1$ (14)	$P12_1/n1$ (14)	$P12_1/n1$ (14)
a [Å]	6.80	6.83	6.80
b [Å]	7.03	7.07	7.02
c [Å]	6.47	6.50	6.47
α [°]	90	90	90
β [°]	103.9	103.3	103.5
γ [°]	90	90	90
$\langle D_V \rangle$ [Å]	57	∞	∞

reveal that the observed XRD pattern is well in accord with a nanocrystalline monazite phase. The fit yields a volume-averaged mean domain size of 5.7 nm which is roughly consistent with the particle size observed in the high-resolution TEM images and shows that the dimensions of the unit cell are similar to those of bulk $LaPO_4$ and bulk $CePO_4$.

Powders of the nanocrystals are easily redispersed in polar solvents. The agglomeration of particles in these solutions was investigated by small-angle X-ray scattering (SAXS) experiments (Kratky compact camera). Figure 3a shows the scattering curve of a colloidal solution containing 0.2 wt% of nanoparticles and a small amount of tetra-*n*-butylammonium hydroxide in 2-propanol. By assuming the scatterers to be homogeneous spheres, the size distribution can be calculated

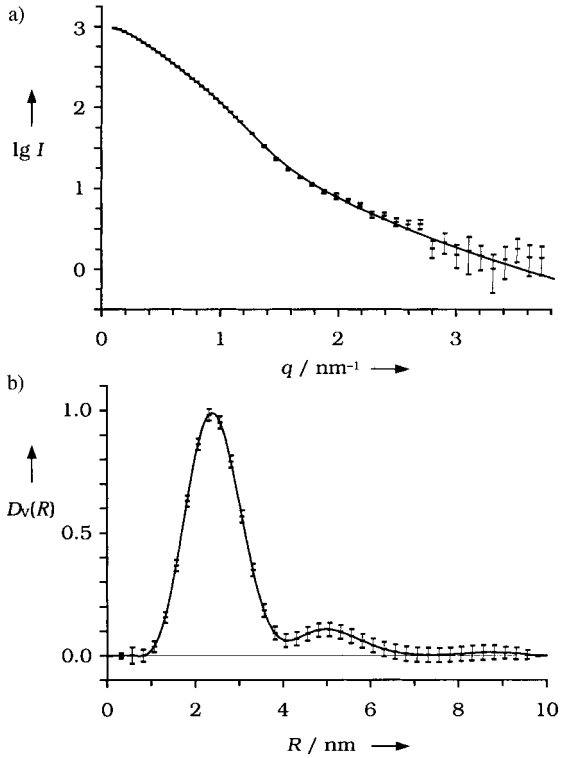

Figure 3. a) Small-angle X-ray scattering (SAXS) curve of a colloidal solution containing 0.2 wt% of $LaPO_4$:Ce,Tb nanoparticles in 2-propanol. The length of the so-called scattering vector q is related to the scattering angle θ, that is, the angle between the directions of incidence and detection, by $q = (4\pi/\lambda_0)\sin(\theta/2)$. $Cu_{K\alpha}$ radiation was used ($\lambda_0 = 0.154$ nm). b) Normalized particle size distribution deduced from the scattering curve by assuming spherical scatterers of radius R.

  1433-7851/01/4003-0574 $ 17.50+.50/0

from the scattering curve by means of the indirect transformation method[10] (ITP-software, University of Graz, Austria). The resulting distribution curve (Figure 3b) shows that most scatterers (90% by volume or 98% by number) have diameters $2R$ below about 8 nm, indicating well-separated particles. The weak additional peak in the distribution curve at about $2R \approx 10$ nm proves that the size of agglomerates is restricted to values below about 15 nm. The position and the width (at half-maximum) of the main peak indicates particle diameters in the range of $2R = 4.8 \pm 1.5$ nm, that is a broader size distribution and a slightly smaller mean particle size than expected from the TEM images. This deviation is very likely caused by the nonspherical shape of many particles which was not accounted for in the calculation of the distribution curve. The high degree of deagglomeration may indicate partial capping of the particle surface by ethylhexanol or ethylhexylphosphate moieties, similar to TOP/TOPO-capped semiconductor nanoparticles.[1a–e] The composition and the properties of the surface of the nanoparticles, however, have not been investigated yet.

The optical properties of $LaPO_4$:Ce,Tb colloids are similar to those of $CePO_4$:Tb nanoparticles[1h] and are determined by transitions between f-electron and d-electron states of cerium and between different f-electron states of terbium, as schematically depicted in Figure 4. Upon UV excitation,

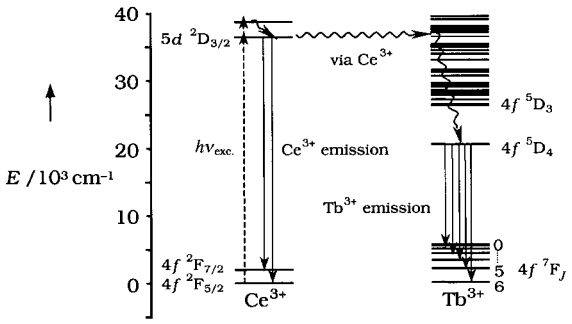

Figure 4. Energy level scheme of $LaPO_4$:Ce,Tb with optical transitions and energy transfer processes as indicated. For simplicity, relaxation of the excited Ce^{3+} state to the lowest vibrational level is not shown in the figure.

colloidal solutions as well as powders of $LaPO_4$:Ce,Tb nanoparticles exhibit strong yellowish-green luminescence (Figure 5) due to transitions between the excited $^5D_4$ state and the ^7F_J ($J = 0-6$) ground states of terbium.[5] The luminescence spectrum shows no significant differences to the spectrum of the bulk material. In fact, particle size effects on the luminescence are expected to be weak, since transitions of the well-shielded f electrons are mainly affected by the local symmetry of the crystal site. In addition to the terbium lines, the luminescence spectrum shows a rather broad emission between about 300 and 400 nm which is caused by the 5d–4f emission of cerium. The cerium emission consists of two transitions from the lowest component of the ^2D state to the spin-orbit components of the ground state, $^2F_{7/2}$ and $^2F_{5/2}$. In contrast to the f electrons of terbium, the d electrons of cerium couple strongly to the lattice phonons resulting in broad overlapping bands and a significant Stokes shift. The latter becomes evident by comparing the fluores-

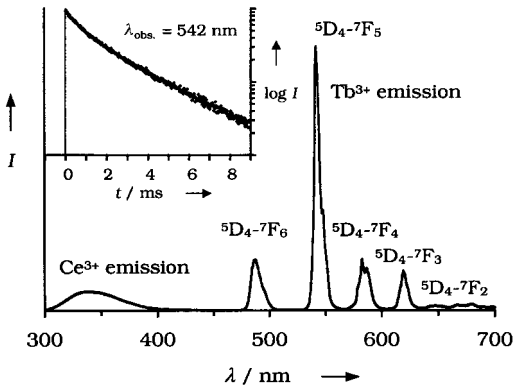

Figure 5. Luminescence spectrum ($\lambda_{exc} = 275$ nm) of a dilute colloid containing about 0.02 wt% of $LaPO_4$:Ce,Tb nanoparticles. Inset: Luminescence decay curve of the same colloid ($\lambda_{exc} = 266$ nm, $\tau_{exc} = 15$ ns; detection wavelength $\lambda_{obs} = 542$ nm).

cence spectrum in Figure 5 with the absorption spectrum of the colloid given as dotted line in Figure 6. Since the spin-orbit components of the excited cerium 5d state, $^2D_{5/2}$ and $^2D_{3/2}$, are strongly split by the crystal field the absorption spectrum shows peaks at 214, 236, 258, and 274 nm. The intensity pattern and the position of the peaks are identical to those

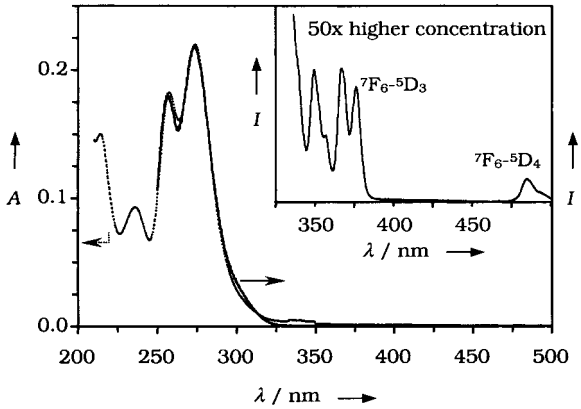

Figure 6. UV/Vis absorption spectrum (dotted line) and luminescence excitation spectrum (solid line, detection wavelength $\lambda_{obs} = 542$ nm) of a dilute colloidal solution containing about 0.02 wt% of $LaPO_4$:Ce,Tb in methanol. Inset: luminescence excitation spectrum ($\lambda_{obs} = 542$ nm) of a solution of higher concentration (50×) displaying transitions from the terbium $^5D_6$ ground state into excited terbium states.

observed in the reflectance and luminescence excitation spectrum of bulk $LaPO_4$:Ce.[11] These features are also observed in the luminescence excitation spectrum of a dilute colloidal solution of the nanoparticles (Figure 6, solid line). The spectrum, monitored at the main terbium line at 542 nm, is identical to the absorption spectrum, verifying energy transfer from Ce^{3+} to Tb^{3+}.[11, 12] Upon UV excitation of the cerium absorption band, a quantum yield of 42% is observed for the terbium emission of $LaPO_4$:Ce,Tb nanoparticles dispersed in a 1:50 mixture of *N*,*N*-dimethylformamide and methanol. If the cerium emission is included, the total quantum yield is 61%, which is among the highest values observed for uncoated nanocrystals. Higher quantum yields have only been reported for semiconductor core–shell nano-

particles,[13] that is, if a sufficiently thick shell of a wide-band gap material with similar lattice constants is grown onto the semiconductor particle cores. This shell reduces luminescence quenching at the particle surface and increases the stability of semiconductor nanoparticles to photochemical corrosion. However, it also complicates the synthesis of larger amounts of material.

Since energy transfer via the particle surface remains possible, the quantum yield of $LaPO_4$:Ce,Tb nanoparticles depends on the solvent and the termination of the particle surface. Due to their large ratio of surface area to volume, nanocrystalline systems are much more strongly influenced by properties of the particle surface than is the case for bulk materials. Particles in methanol containing some tetra-*n*-butylammonium hydroxide, for instance, show a reduced quantum yield upon UV excitation of the cerium band of $\phi = 17\,\%$ and $\phi = 24\,\%$ for the terbium and the total emission, respectively. Since the cerium emission and the terbium emission are both reduced by the same factor (0.4), we have to assume that the excited state of cerium is not only depleted by energy transfer to terbium but also by a competing process involving the solvent or the base used. In fact, the luminescence quantum yield of organometallic cerium complexes[14] is known to depend on the ligands binding to the cerium atom. Even for cerium complexes, however, the quenching mechanism seems to be not very well understood.[14] Therefore, we are presently investigating the influence of surface modifications on the luminescence quantum yield of the particles.

In contrast to the optically allowed d–f transitions of cerium, transitions from the terbium $^7F_6$ ground state into the higher excited terbium states are spin- and parity-forbidden and are only observed in the luminescence excitation spectrum of rather concentrated colloidal solutions (inset of Figure 6). The low transition probabilities of the terbium f–f transitions are also reflected in their long luminescence lifetime. The luminescence decay curve of the colloid (inset of Figure 5) shows a lifetime in the range of 3–4 ms, that is a value similar to the 3.2 ms observed for the bulk material.[11, 12]

The kinetics of the luminescence decay deviates slightly from single-exponential behavior. This can be explained by energy transfer from the excited state of terbium to quencher ions as recently discussed for $CePO_4$:Tb nanoparticles.[1h] The origin and the exact nature of these quenchers is not yet understood. However, if energy transfer from the excited terbium state could be reduced even higher quantum yields of the terbium emission may be achieved.

Experimental Section

Synthesis: Tris(ethylhexyl)phosphate (300 mL) was purged with dry nitrogen and a solution containing $LaCl_3 \cdot 7H_2O$ (7.43 g, 20 mmol), $CeCl_3 \cdot 7H_2O$ (8.38 g, 22.5 mmol), and $TbCl_3 \cdot 6H_2O$ (2.80 g, 7.5 mmol) in methanol (100 mL) was added. Then, water and methanol were distilled off by heating the solution to 30–40 °C in vacuum. A freshly prepared solution of crystalline phosphoric acid (4.90 g, 50 mmol) dissolved in a mixture of trioctylamine (65.5 mL, 150 mmol) and tris(ethylhexyl)phosphate (150 mL) was added. The clear solution was repeatedly evacuated and purged with nitrogen in order to minimize oxidation of Ce^{3+} to Ce^{4+} at elevated temperatures, and was subsequently heated at 200 °C. During heating, some of the phosphoric acid ester was cleaved and the boiling point of the colloid decreased slowly. Heating was stopped when the temperature had dropped to about 170–175 °C (after about 30 to 40 h). After the mixture had been cooled to room temperature, a fourfold excess of methanol was added to the transparent colloid, resulting in precipitation of the nanocrystals. The latter were separated by centrifugation, washed with methanol, and dried. (Yield: 10.8 g, 89 %).

Transparent and scatter-free colloidal solutions were obtained by redispersing the powder (50 mg) either in *N*,*N*-dimethylformamide (5 mL) at 100 °C or in methanol (5 mL) containing a few drops of a 25 wt % solution of tetra-*n*-butylammonium hydroxide in methanol. Before spectroscopic measurements, both solutions were diluted with methanol or 2-propanol by a factor of 50.

The room-temperature quantum yields of the colloids were determined by comparing the emission of the colloidal solution with the emission of a solution of rhodamine 6G (Lambda Physics, laser grade; in spectroscopic grade ethanol) of identical optical density at the excitation wavelength.

Received: May 2, 2000
Revised: Otober 17, 2000 [Z15056]

[1] a) C. B. Murray, D. J. Norris, M. G. Bawendi, *J. Am. Chem. Soc.* **1993**, *115*, 8706; b) T. J. Trentler, T. E. Denler, J. F. Bertone, A. Agrawal, V. L. Colvin, *J. Am. Chem. Soc.* **1999**, *121*, 1613; c) O. I. Micic, C. J. Curtis, K. K. Jones, J. R. Sprague, A. J. Nozik, *J. Phys. Chem.* **1994**, *98*, 4966; d) A. A. Guzelian, J. E. B. Katari, A. V. Kadavanich, U. Banin, K. Hamad, E. Juban, A. P. Alivisatos, R. H. Wolters, C. C. Arnold, J. R. Heath, *J. Phys. Chem.* **1996**, *100*, 7212; e) A. A. Guzelian, U. Banin, A. V. Kadavanich, X. Peng, A. P. Alivisatos, *Appl. Phys. Lett.* **1996**, *69*, 1432; f) M. A. Hines, P. Guyot-Sionnest, *J. Phys. Chem. B* **1998**, *102*, 3655; g) J. Rockenberger, E. C. Scher, A. P. Alivisatos, *J. Am. Chem. Soc.* **1999**, *121*, 11596; h) K. Riwotzki, H. Meyssamy, A. Kornowski, M. Haase, *J. Phys. Chem. B* **2000**, *104*, 2824.

[2] X. Peng, J. Wickham, A. P. Alivisatos, *J. Am. Chem. Soc.* **1998**, *120*, 5343.

[3] G. Blasse, B. C. Grabmaier, *Luminescent Materials*, Springer, Berlin, **1994**.

[4] N. Hashimoto, Y. Takada, K. Sato, S. Ibuki, *J. Lumin.* **1991**, *48–49*, 893.

[5] B. M. J. Smets, *Mater. Chem. Phys.* **1987**, *16*, 283.

[6] a) M. Bruchez, Jr., M. Moronne, P. Gin, S. Weiss, A. P. Alivisatos, *Science* **1998**, *281*, 2013; b) W. C. W. Chan, S. Nie, *Science* **1998**, *281*, 2016.

[7] a) V. L. Colvin, M. C. Schlamp, A. P. Alivisatos, *Nature* **1994**, *370*, 354; b) B. O. Daboussi, M. G. Bawendi, O. Onitsuka, M. F. Rubner, *Appl. Phys. Lett.* **1995**, *66*, 1316; c) Y. Yang, J. Huang, S. Liu, J. Shen, *J. Mater. Chem.* **1997**, *7*, 131; d) M. C. Schlamp, X. Peng, A. P. Alivisatos, *J. Appl. Phys.* **1997**, *82*, 5837.

[8] X. Peng, J. Wickham, A. P. Alivisatos, *J. Am. Chem. Soc.* **1998**, *120*, 5343.

[9] a) R. X. Fischer, C. Lengauer, E. Tillmanns, R. J. Ensink, C. A. Reiss, E. J. Fantner, *Mater. Sci. Forum* **1993**, *133–136*, 287; b) R. A. Young, *The Rietveld Method*, Oxford University Press, Oxford, **1993**.

[10] a) O. Glatter, *J. Appl. Crystallogr.* **1980**, *13*, 7; b) O. Glatter, *Acta Phys. Austriaca* **1977**, *47*, 83; c) O. Glatter, *J. Appl. Crystallogr.* **1977**, *10*, 415.

[11] J.-C. Bourcet, F. K. Fong, *J. Chem. Phys.* **1974**, *60*, 34.

[12] W. van Schaik, S. Lizzo, W. Smit, G. Blasse, *J. Electrochem. Soc.* **1993**, *140*, 216.

[13] a) A. R. Kontan, R. Hull, R. L. Opila, M. G. Bawendi, M. L. Steigerwald, P. J. Carroll, L. E. Brus, *J. Am. Chem. Soc.* **1990**, *112*, 1327; b) C. F. Hoener, K. A. Allan, A. J. Bard, A. Campion, M. A. Fox, T. E. Mallouk, S. E. Webber, J. M. White, *J. Phys. Chem.* **1992**, *96*, 3812; c) M. Danek, K. F. Jensen, C. B. Murray, M. G. Bawendi, *Chem. Mater.* **1996**, *8*, 173; d) M. A. Hines, P. Guyot-Sionnest, *J. Phys. Chem.* **1996**, *100*, 468; e) O. I. Micic, J. R. Sprague, Z. Lu, A. J. Nozik, *Appl. Phys. Lett.* **1996**, *68*, 3150; f) X. Peng, M. C. Schlamp, A. V. Kadavanich, A. P. Alivisatos, *J. Am. Chem. Soc.* **1997**, *119*, 7019; g) B. O. Dabbousi, J. Rodriguez-Viejo, F. V. Mikulec, J. R. Heine, H. Mattoussi, R. Ober, K. F. Jensen, M. G. Bawendi, *J. Phys. Chem. B* **1997**, *101*, 9463.

[14] S. T. Frey, W. De Horrocks, Jr., *Inorg. Chem.* **1991**, *30*, 1073.

  1433-7851/01/4003-0576 $ 17.50+.50/0